NASA/TM—2003-212738

# Development of a High-Pressure Gaseous Burner for Calibrating Optical Diagnostic Techniques

Jun Kojima and Quang-Viet Nguyen
Glenn Research Center, Cleveland, Ohio

December 2003

The NASA STI Program Office . . . in Profile

Since its founding, NASA has been dedicated to the advancement of aeronautics and space science. The NASA Scientific and Technical Information (STI) Program Office plays a key part in helping NASA maintain this important role.

The NASA STI Program Office is operated by Langley Research Center, the Lead Center for NASA's scientific and technical information. The NASA STI Program Office provides access to the NASA STI Database, the largest collection of aeronautical and space science STI in the world. The Program Office is also NASA's institutional mechanism for disseminating the results of its research and development activities. These results are published by NASA in the NASA STI Report Series, which includes the following report types:

- TECHNICAL PUBLICATION. Reports of completed research or a major significant phase of research that present the results of NASA programs and include extensive data or theoretical analysis. Includes compilations of significant scientific and technical data and information deemed to be of continuing reference value. NASA's counterpart of peer-reviewed formal professional papers but has less stringent limitations on manuscript length and extent of graphic presentations.

- TECHNICAL MEMORANDUM. Scientific and technical findings that are preliminary or of specialized interest, e.g., quick release reports, working papers, and bibliographies that contain minimal annotation. Does not contain extensive analysis.

- CONTRACTOR REPORT. Scientific and technical findings by NASA-sponsored contractors and grantees.

- CONFERENCE PUBLICATION. Collected papers from scientific and technical conferences, symposia, seminars, or other meetings sponsored or cosponsored by NASA.

- SPECIAL PUBLICATION. Scientific, technical, or historical information from NASA programs, projects, and missions, often concerned with subjects having substantial public interest.

- TECHNICAL TRANSLATION. English-language translations of foreign scientific and technical material pertinent to NASA's mission.

Specialized services that complement the STI Program Office's diverse offerings include creating custom thesauri, building customized databases, organizing and publishing research results . . . even providing videos.

For more information about the NASA STI Program Office, see the following:

- Access the NASA STI Program Home Page at ***http://www.sti.nasa.gov***

- E-mail your question via the Internet to help@sti.nasa.gov

- Fax your question to the NASA Access Help Desk at 301–621–0134

- Telephone the NASA Access Help Desk at 301–621–0390

- Write to:
  NASA Access Help Desk
  NASA Center for AeroSpace Information
  7121 Standard Drive
  Hanover, MD 21076

NASA/TM—2003-212738

# Development of a High-Pressure Gaseous Burner for Calibrating Optical Diagnostic Techniques

Jun Kojima and Quang-Viet Nguyen
Glenn Research Center, Cleveland, Ohio

Prepared for the
2003 American Flame Research Committee International Symposium on
Combustion Research and Industrial Practice: Bridging the Gap
cosponsored by the American Flame Research Committee (AFRC) and the
Combustion Research Facility of Sandia National Laboratory
Livermore, California, October 16–17, 2003

National Aeronautics and
Space Administration

Glenn Research Center

December 2003

**Acknowledgments**

The authors acknowledge Mr. Gregg Calhoun, Mr. William Thompson, Mr. Raymond Lotenero, and Mr. Gary Lorenz for their assistance in the construction and operation of the facilities. We also acknowledge Mr. Anthony Iannetti for his efforts in providing the NCC simulations for this burner.



Available from

NASA Center for Aerospace Information
7121 Standard Drive
Hanover, MD 21076

National Technical Information Service
5285 Port Royal Road
Springfield, VA 22100

Available electronically at http://gltrs.grc.nasa.gov

# Development of a High-Pressure Gaseous Burner for Calibrating Optical Diagnostic Techniques

Jun Kojima* and Quang-Viet Nguyen†
National Aeronautics and Space Administration
Glenn Research Center
Cleveland, Ohio 44135

## Abstract

In this work-in-progress report, we show the development of a unique high-pressure burner facility (up to 60 atm) that provides steady, reproducible premixed flames with high precision, while having the capability to use multiple fuel/oxidizer combinations. The high-pressure facility has four optical access ports for applying different laser diagnostic techniques and will provide a standard reference flame for the development of a spectroscopic database in high-pressure/temperature conditions. Spontaneous Raman scattering (SRS) was the first diagnostic applied, and was used to successfully probe premixed hydrogen-air flames generated in the facility using a novel multi-jet micro-premixed array burner element. The SRS spectral data include contributions from $H_2$, $N_2$, $O_2$, and $H_2O$ and were collected over a wide range of equivalence ratios ranging from 0.16 to 4.9 at an initial pressure of 10-atm via a spatially resolved point SRS measurement with a high-performance optical system. Temperatures in fuel-lean to stoichiometric conditions were determined from the ratio of the Stokes to anti-Stokes scattering of the *Q*-branch of $N_2$, and those in fuel-rich conditions via the rotational temperature of $H_2$. The SRS derived temperatures using both techniques were consistent and indicated that the flame temperature was approximately 500 K below that predicted by adiabatic equilibrium, indicating a large amount of heat-loss at the measurement zone. The integrated vibrational SRS signals show that SRS provides quantitative number density data in high-pressure $H_2$-air flames.

## Introduction

The experimental testing of aircraft engine hardware is becoming prohibitively expensive. Sometimes more important than the cost of testing, the development time for an engine can sometimes take upwards of 10 years or more. In order to reduce the costs associated with engine development and to reduce the time-to-market of new engine concepts, industry is relying more and more on computational modeling of the engines as an alternative to testing before actual hardware is built. The quantitative measurement of species concentration and/or temperature in high-pressure combustion environments is, in

*National Research Council—NASA Resident Research Associate at Glenn Research Center; E-mail: Jun.Kojima@grc.nasa.gov
†E-mail: Quang-Viet.Nguyen@nasa.gov

fact, of prime importance to validate and anchor the current suite of computational models of gas turbine combustion. Non-intrusive optical diagnostics are becoming more and more relied upon for code-validation purposes. The application of laser spectroscopic diagnostics such as laser-induced fluorescence (LIF), SRS, or laser absorption spectroscopy in high-pressure flames is one of the major challenges in the code validation process for advanced combustors. We are particularly interested in measuring the entire Raman spectral response in a variety of high-pressure flames (up to 60 atm) with various fuels ($H_2$, $H_2$-CO, $CH_4$, and jet-A) and oxidizers (Air, $O_2$). In an effort to develop a SRS spectral database in hydrocarbon flames, we are first examining simple $H_2$-Air flames in detail before moving on to fuels containing carbon.

High-density gases in high-pressure cells [1-2] are typically used to study fundamental aspects of laser diagnostics such as the pressure dependence on spectral shapes or quenching effects. Real combustion experiments, however, are necessary to look into details about such molecular spectroscopic phenomena over the range of combustion pressure, temperature, and species composition. Thus, a high-pressure burner that can serve as a precision calibration standard would be of great use to the combustion research community. Such a burner should provide a stable and repeatable source of combustion products over a wide operational range. In the past, water-cooled sintered-metal porous plate flat-flame burners (so-called McKenna burners) have been used for studies of high-pressure laminar hydrocarbon flames [3-5]. This type of burner was reported to work well in providing stabilized high-pressure flames at pressures up to 60 atm for hydrocarbon flames, and is useful for optical calibrations at reduced flame temperatures [6]. However, this type of burner suffers from a large amount of heat loss due to the short distance (generally, < 1 mm) between the water-cooled burner surface and the flat-flame. This type of burner also suffers from flame temperatures that decrease with increasing pressures due to a reduction in burner surface-to-flame distance caused by the higher pressures [5]. Furthermore, the low flow velocities through the sintered plate produce a flame that is susceptible to the increased effects of buoyancy at high pressures. As for hydrogen flames, sintered bronze-matrix burner have been proposed to provide a 15-bar $H_2$-air laminar premixed flame for the calibration of CARS diagnostics, albeit with the risk of thermal meltdown even in fuel-rich ($> \phi = 3.5$) conditions [7]. Despite these drawbacks, the McKenna burner has been a popular burner for high pressure studies. However, if higher flame temperatures are required, and they are indeed necessary for the SRS calibration procedure since the spectral interferences among different species generally become stronger at higher temperatures, then a different type of burner must be used.

The alternative is the so-called Hencken burner operated in a non-premixed mode with multiple fuel tubes is generally used for optical calibration in $H_2$ flames [6]. This type of burner works well at atmospheric pressure conditions and is able to provide near adiabatic flames over a wide range of equivalence ratios, however, flow-field uniformity and the uncertainty in flow rates are still an issue [6]. However, the Hencken burner cannot survive a high pressure hydrogen-air flame due to thermal meltdown, and cannot be operated in a premixed mode with hydrogen due to flash-back.

The burner design that we developed as an alternative, is a versatile high-pressure burner that can operate over a wide range of temperature, pressures, equivalence ratios, and with different fuels and oxidizers. In this paper, we first describe our burner design

in some detail. We then present the results from a series of SRS measurements applied to this burner for a 10-atm $H_2$-air premixed flame over the equivalence ratios ranging from $\phi$ = 0.2 to 5.0 to demonstrate a capability of the burner.

## High-Pressure Burner

The primary goal of our research burner design is to generate a stable and precisely controllable stream of combustion products for calibrating optical diagnostic techniques. The ease of manufacturing and testing durability is of prime importance in addition to the following requirements:

1. Versatile operation: Premixed or Non-premixed
2. Multi-fuel capability ($H_2$, Hydrocarbon, Jet-A, spray fuel)
3. Pressure range up to 60 atm
4. Self-cooling without using water
5. Stable operation over a wide range of equivalence ratios
6. Low cost

*Burner Nozzle Design*

The design of a burner capable of satisfying the above requirements without flash-back is indeed challenging. The burner design is based on a premixed concept that also utilizes back-side impingement cooling and micro-mixing at high velocities to overcome these challenges.

Figure 1 shows a schematic of the micro-premixed burner design. Basically, the burner consists of an array of closely-spaced premixed fuel/oxidizer jets that issue from the burner face and quickly combine downstream of the face to form a uniform flow pattern. The fuel/oxidizer premixing occurs via micro-mixing just upstream of the burner face in a thin cavity just before the flows exit the burner face. An array of 7 x 7 fuel tubes and 8 x 8 oxidizer tubes approximately 1 mm in diameter in a staggered arrangement provides the flows to the thin premixing cavity. The oxidizer flow first impinges on the backside of the burner face and then turn 90 degrees to effect the micro-mixing with the fuel jets. The mixing is also enhanced by the large shear forces induced in the sudden directional change of the oxidizer flows. The premixed fuel/oxidizer jets then exit through an array of 7 x 7 premix holes that are coaxially aligned with the fuel-tube supply array. These premixed jets have an approximately 1:5 expansion ratio to slow the jet velocities down from the high velocities through the nozzle throat required to prevent flash-back. The premixed jet array is approximately 18 x 18 mm in size. These 49 jets then continue to mix and combine to become a single uniform flame downstream of the burner face. By mixing the fuel and oxidizer just upstream of the burner face in a region of high gas velocity, flashback into the thin premixing chamber is avoided if the bulk velocity is kept above the laminar flame speed of the fuel-air mixture (which can be as high as 10 m/s for high pressure $H_2$-air flames).

By impingement cooling the burner face with the oxidizer flow, the burner can be operated without any water cooling, and this helps to keep the flame temperatures high. The burner produces a region of combustion products directly downstream of a premixed flame with a uniform flow pattern over an approximate 5 x 5 mm zone. The copper burner face also is cooled to a certain degree by convection to the gases in the mixing holes as well as the direct conduction to the main burner body. At equivalence ratios

below 0.6 the burner can be operated indefinitely; at higher equivalence ratios, the burner can be operated for typically 2 minutes before the burner face temperatures (sensed by thermocouples) get too hot (920 K). However, this is not a problem as only about 30 seconds of run time is needed to acquire the Raman scattering data. Note no preheat air-fuel mixture was fed to the burner even for a lean flame in this experiment.

**Facility**

Figure 2 shows a schematic of the high-pressure burner rig and gas flow system. The burner nozzle is mounted inside the air-cooled combustion liner casing of the high-pressure rig. The pressure inside the casing is the same as for the rig. The following sections describe the different aspects of the facility.

*Rig Pressure*

The rig pressure can range from 1 atm to 60 atm. The rig pressure was automatically maintained with a stand-alone PID-process controller that regulates a back-pressure valve to stabilize the pressure fluctuations to better than ± 1 % for each condition.

*Cooling Air*

For rig pressure below 30 atm, ambient-temperature cooling air is supplied from a central facility compressor and is introduced in two locations: at the bottom of the rig for cooling the combustion liner (≤ 6.8 kg/min) and downstream of the liner to quench-cool the combustion by-products (≤ 5.5 kg/min). For rig pressures above 30 atm, the cooling air is provided by a large trailer-mounted array of high pressure air cylinders. The cooling airflow was controlled to within 3% accuracy using remotely operated pressure regulators in conjunction with non-critical flow venturi meters. The mass flow rates of the two cooling air flows were typically the same. Ten percent or less of the total cooling flow rate of the facility air was used as a purge-air for the optical windows during experiments prevent water vapor condensation. A small amount of cooling bleed air was fed into the casing to avoid building up of combustion products around the burner.

*Hydrogen (Fuel) Systems*

A remotely controlled flow delivery system is required to accurately meter the flow rates for the gaseous hydrogen fuel at various operating conditions ranging from fuel-lean to fuel-rich. Flows ranged from 50 standard liters/min (SLM) to 580 SLM. The $H_2$ flows were metered using a bank of 3 critical flow venturis fitted with pressure transducers; the bank of meters allows a wide dynamic range of flow rates to be metered with high accuracy. An accuracy of better than 1% was achieved for the flow rate measurement using calibrated (NIST-traceable) critical flow venturi meters. The sonic flow venturis also serve to limit the maximum flow of the $H_2$ in case of a downstream drop in rig pressure (as in the case of a burst disc rupture event). The use of critical flow venturi meters ensures that the mass flow rate stays constant regardless of pressure fluctuations in the rig. The upstream $H_2$ pressure was controlled with an automatic process control system which actuates a precision dome-loaded pressure regulator. The $H_2$ gas was provided by 12-pack cylinder arrays at 150 atm pressure located on a pallet outside of experimental test cell.

*Air (Oxidizer) Systems*
The air system is almost identical to the gaseous fuel system except the flows range from 200 SLM to 4600 SLM.

*Ignition System*
A retractable, high-energy surface-discharge aircraft style igniter system is used to ignite the burner. The igniter is inserted to a radial location above the burner using a geared stepper motor, and a 10-spark sequence is then initiated prior to opening the $H_2$ flow valves to introduce the fuel flow.

*Facility Parameters*
Critical facility data was logged using a computer at 1 second intervals (minimum) with 16-bit precision. Data points were stored to computer disk with the choice of averaging over arbitrary *n*-points or an instantaneous record mode. Those parameters include all pressures, temperatures, and flow rates described above.

*Remote Control System*
The facility and all gas flows were controlled and operated through a computer touch-screen human-machine-interface (HMI) via a computer controlled interface using the In-Touch Software Systems' 'Wonderware' package in conjunction with a programmable logic controller (PLC). Manually set actuators and valves were for facility startup only and all actuators/valves that need to be controlled during run time were via the HMI system. The CCD camera for the Raman data collection was also remotely operated via network-based Windows software.

*Shutdown System*
In a high-pressure, hydrogen-air combustion experiment, safety is as important as the accuracy of the experiments. A burst disk (64 atm) located between the main pressure chamber and the exhaust pipe is used to relieve the chamber pressure in case of the unlikely event of a detonation or explosive event. We also implemented a comprehensive shutdown system for the facility using the PLC as follows. Firstly, manual shutdown can be effected by closing fuel and then oxidizer flows gradually. Secondly, shutdown should be instigated automatically via PLC in the event of:
(1) Flameout detection via low temperature on a flame sensor thermocouple (TC) or via visual means; (2) Rig over-temperature on a rig TC; (3) Burner hardware over-temperature on a burner face TC; (4) Gas leak detected for fuel the supply system via electrochemical leak sensors in both the fuel systems gas cabinet or in the test cell; (5) Low air cooling flow condition; (6) Low fuel/oxidizer supply pressure; (7) Any anomalous behavior of burner operation as determined by the qualified operator. A minimum mass flow rate of total cooling air for the rig was set at 1.36 kg/min in order to prevent a lower explosion limit (LEL) from being reached in case of a flame-out.

## Raman Diagnostics and Experiment

To determine temperature and major species, multiple spontaneous rotational-vibrational Raman scattering spectra were measured via a spatially-resolved, point laser Raman system. An injection seeded, Q-switched Nd:YAG laser operating at 532 nm with about 1000 mJ/pulse was used as the excitation laser source. The laser pulse width at FWHM was measured to be 8.4 ns. The injection seeding feature helps to produce a better pulse-to-pulse energy stability with less timing-jitter. Each pulse from the laser was temporally "stretched" to a longer pulse (75 ns halfwidth) by means of the pulse stretching optics [8] with 83% energy throughput. The pulse stretcher reduces the peak power to approximately 10% of the input peak power so that the laser pulse can be focused into the fine volume without the breakdown of gases as well as without damaging windows. Note that the breakdown of the air at high-pressure circumstances can be more significant because breakdown power threshold for the air has negative pressure dependence. Using a 750 mm focal length lens, the light emerging from pulse stretcher was focused to a beam waist at the probe volume. The probe volume size is approximately 0.5 mm in diameter and 1.6 mm in long. The beam, after passing through the probe volume, was then reflected back into the probe volume using a 400 mm collimating lens and a right-angle prism; this effectively doubled the laser energy in the probe volume.

The vertically polarized Raman scattering light was collected at a 90-degree angle with a camera lens (85 mm, f/1.4) and was then focused onto a single silica optical fiber (400 μm in core diameter) connected to a electro-mechanical high-speed shutter [9] for gating the light. The shutter system, which provided 24 μs exposure (FWHM) with 0.4 μs jitter with 12 x 0.762 mm clear aperture to reduce the effects of background light interferences. The gated light from the shutter was directed to the spectrograph. The optical throughput of the shutter system was 55% including fiber transmission losses. The axially transmissive spectrograph (f/1.8) is fitted with a holographic notch filter to attenuate the Rayleigh scattering component of the signal by over six orders of magnitude. A volume holographic transmission grating disperses the signal into different wavelengths which are detected by a non-intensified, liquid nitrogen cooled, backside-illuminated CCD camera (1340 x 100 pixels). The electronic exposure of the CCD was 5 ms (but the actual time exposure limited by the shutter is 24 μs), and the data was accumulated for 300 shots (on the chip) to increase the signal-to-noise. The spectral resolution was 1.2 nm for the 100 μm slit used. The spectral intensity was calibrated by a NIST-traceable blackbody lamp. Raman scatterings were measured at 25 mm above the burner nozzle surface on the center axis.

The high-pressure rig was fitted with four 44 mm thick UV grade fused silica windows with a clear aperture of 85 mm for optical diagnostics. One port was used for a video camera to record and monitor the burner operation. The other three windows were used as laser beam inlet ports, and laser scattering detection port. The burner housing was hydro-tested to 34 atm with burner face blank insert, and was rated for operation up to 14 atm differential pressure at 920 K with the actual perforated burner face. In this study, the rig was operated at a nominal pressure of 10 atm.

## Results and Discussion

Figure 3 shows photographs of 10-atm $H_2$-air flames at $\phi = 0.6$, 1.0, and 3.2 with an exposure time of 3 seconds. The luminous zones in the photographs indicate the major combustion product – water in this case. According to the photographs, the burner generates multiple small hydrogen premixed flames just above the burner face. The burned gases combine downstream to deliver a homogeneous zone of combustion products. The luminous zone appears different in size and shape depending on the equivalence ratio. The flow rate of the gases was not fixed in the current experiment, so the mean flow velocity at the burner port was different for each equivalence ratio. The rich flame ($\phi = 3.2$) has more residual un-burned hydrogen in the post flame gases than the stoichiometric or lean cases. Thus, the un-burned hydrogen continues to react over a wider reaction zone downstream of the burner, resulting in a diverging luminous flame zone as shown in Fig. 3c. Therefore, measurements for the purpose of the optical calibration are necessary at a point just above the primary flame zone. The current measurement height, which can be seen in the picture as a background fiber core image, seems to be still in a homogeneous stream of combustion gases. Further discussion about flows and distributions of combustion products could be made via flow visualization and/or planar imaging techniques.

To obtain quantitative information on basic characteristics of the burner we measured SRS data from $H_2$, $H_2O$, $N_2$, and $O_2$ over a wide range of equivalence ratios. Figure 4 shows entire Raman spectra of major species in $H_2$-air combustion at 10 atm (300-shot averaged). The SNR of these spectra is about 10,000:1, sufficient to allow good-quality analysis of temperature and species concentrations. Because Raman scattering intensity increases linearly with pressure, Raman spectroscopic techniques have an advantage in high-pressure or high-density studies. In a lean flame ($\phi = 0.16$), a higher intensity of $O_2$, and $N_2$ signals are observed than in the other flames, while strong rotational and vibrational lines of $H_2$ are observed in a highly rich flame ($\phi = 4.9$). In a stoichiometric flame ($\phi = 1.03$), the anti-Stokes branch of $N_2$ Raman appears, which indicates a higher temperature.

Temperatures at each equivalence ratio were calculated by either the anti-Stokes/Stokes ratio of $N_2$ spectra [10] or rotational spectrum distribution of $H_2$ [11]. The measurement uncertainty of $H_2$ rotational temperature is 8% maximum for a lean flame and 1% maximum for a rich flame. The results are shown in Fig. 5. The adiabatic temperature was calculated using NASA Glenn Chemical Equilibrium (CEA) Code [12]. Experimentally determined temperatures via the different spectroscopic techniques agreed well, especially in rich flame cases. Since uncertainty of the rotational $H_2$ temperature increases in stoichiometric or lean flames due to the lower $H_2$ signal intensity, the mismatches between $N_2$ Raman temperature and $H_2$ temperature between $\phi = 0.7$ to 1.5 do not necessarily mean a non-thermal equilibrium between two molecules. The non-equilibrium condition, generally, is not likely in high-pressure combustion due to a quite small collisional time scale [13-14]. Based on the signal-to-noise ratio, $N_2$-based analyses are more accurate for flames with $\phi < 2.0$, whereas $H_2$-based analyses are more accurate for flames with $\phi > 2.0$. Overall variation of anti-Stokes/Stokes temperature with $\phi$ was qualitatively the same as the variation of the adiabatic temperature. The

temperature difference between experiment and calculation by more than 500 K indicates that a large amount of heat loss is occurring in the stoichiometric and rich flames at the measurement location (25 mm above the burner face). We attribute the large amount of heat loss to the following causes: (1) near-infrared/infrared radiation emitted by the main combustion products such as $H_2O$ at this temperature; (2) possible cold air entrainment and dilution in the post flame zone at this axial location; (3) and for the stoichiometric flame, additional heat losses to the burner face through radiation or conduction, as evidenced by the brightly glowing central burner face element. One possible solution to reduce the effects of the heat loss is to move the measurement location closer to the burner face. Our preliminary analysis of the burner element using a comprehensive CFD code with finite-rate $H_2$-Air chemistry indicates that the primary flame zone may be located as low as 1 mm above the burner face [15].

The variation of measured species concentration ($H_2$, $H_2O$, $O_2$, $N_2$) with equivalence ratio is shown in Fig. 6 along with calculated chemical equilibrium (at measured temperature) species concentration. Experimental data were derived from intensity integrated (pixel integration) contribution of each vibrational Raman spectrum for each molecule and were not calibrated to absolute number density but based on the quantitative measurements. Calculated results were shown in the figure to fit to the experimental data for the comparison. The experimental profile of species number density agrees reasonably well with the calculated results in the high-pressure flames: the $H_2O$ profile has a peak concentration around stoichiometry ($\phi = 1.0$) which is also indicated by calculation; $O_2$ concentration decreases with $\phi$ then becomes almost zero at $\phi > 1.0$ as the calculated result shows; $N_2$ also is in good agreement. We, however, found a difference between experimental and computational result in $H_2$ concentration while their general trends are the same. The data shows a slightly higher amount of $H_2$ and this may result from some residual un-burned hydrogen in the post flame zone in the lean flames, or it may be the result of a spectroscopic interference that needs to be accounted for using exactly the calibration techniques we are pursuing in this effort.

## Summary

We developed and tested a novel high-pressure micro-premixed burner design that utilizes an array of closely-spaced small premixed flames for calibrating optical diagnostics in high-pressure flames. The new high pressure burner produces steady, reproducible premixed flames with high precision, and has the ability to use multiple fuel/oxidizer combinations. Direct observations of flame luminescence at different equivalence ratios showed that the array of small premixed flames generate a homogeneous zone of hot combustion products downstream of the burner face. From the initial test results, this burner appears to be a good candidate for a reference burner to be used for calibrating optical diagnostic techniques. To demonstrate the performance of the burner, SRS data from $H_2$, $N_2$, $O_2$, and $H_2O$ were measured in a 10-atm $H_2$-air premixed flame over the wide range of equivalence ratios ($\phi = 0.16$ to 4.9). Temperatures were determined from Stokes/anti-Stokes $N_2$ spectra as well as from rotational $H_2$ spectra (in rich flames). Major species concentrations were also determined from each vibrational Raman spectrum. Experimentally determined temperature and species profiles over the

range of equivalence ratio were compared with computational results via an adiabatic chemical equilibrium code. The results showed that combustion products produced by our high-pressure burner behaved in a reasonably predictable manner. However, it appears that the expectation of a fully-reacted combustion zone was not achieved according to the residual $H_2$ Raman signals at fuel-lean conditions. Additionally, the temperature of the combustion products is far below adiabatic equilibrium. Based on these findings, further experimental efforts to measure temperature and species at different burner heights are necessary. Additional computational study of the flow field including mixing conditions and temperature distributions for this burner are also in progress.

## References


[1] Y. Gu, Y. Zhou, H. Tang, E.W. Rothe, and G.P. Reck, "Pressure Dependence of Vibrational Raman Scattering of Narrow-Band, 248-nm, Laser Light by $H_2$, $N_2$, $O_2$, $CO_2$, $CH_4$, $C_2H_6$, and $C_3H_8$ as High as 97 bar," *Appl. Phys. B* **71**, 865–871, (2000).

[2] V. Nagali and R.K. Hanson, "Design of a Diode-laser Sensor to Monitor Water Vapor in High-Pressure Combustion Gases," *Appl. Opt.* **36**, 9518–9527, (1997).

[3] C. Schulz, V. Sick, U.E. Meier, J. Heinze, and W. Stricker, "Quantification of NO A-X(0,2) Laser-Induced Fluorescence: Investigation of Calibration and Collisional Influences in High-Pressure Flames," *Appl. Opt.* **38**, 1434–1443, (1999).

[4] W.G. Bessler, C. Schulz, T. Lee, J.B. Jeffries, and R.K. Hanson, "Strategies for Laser-Induced Fluorescence Detection of Nitric Oxide in High-Pressure Flames. I. A-X(0,0) Excitation," *Appl. Opt.* **41**, 3547–3557, (2002).

[5] T.S. Cheng, T. Yuan, C.-C. Lu, and Y.-C. Chao, "The Application of Spontaneous Vibrational Raman Scattering for Temperature Measurements in High Pressure Laminar Flames," *Combust. Sci. Technol.* **174**, 111–128, (2002).

[6] R.S. Barlow, C.D. Carter, R.W. Pitz, "Chapter 14: Multiscalar Diagnostics in Turbulent Flames," *Applied Combustion Diagnostics* (ed. K. Kohse-Hoinghaus and J. B. Jeffries), Taylor & Francis, London, 400-401.

[7] J. Hussong, R. Lückerath, W. Stricker, X. Bruet, P. Joubert, J. Bonammy, and D. Robert, "Hydrogen CARS Thermometry in High-Pressure $H_2$-Air Flame. Test of $H_2$ Temperature Accuracy and Influence of Line Width by Comparison with $N_2$ CARS as Reference," *Appl. Phys. B* **73**, 165–172, (2001).

[8] J. Kojima, and Q.V. Nguyen, "Laser Pulse-Stretching Using Multiple Optical Ring-Cavities," *Appl. Opt.* **41**, 6360–6370, (2002).

[9] Q.V. Nguyen, "High Speed Electromechanical Shutter for Imaging Spectrographs," NASA owned intellectual property, patent pending, (2001).

[10] S.M. Schoenung, R.E. Mitchell, "Comparison of Raman and Thermocouple Temperature Measurements in Flames" *Combust. Flame* **35**, 207–211 (1979).

[11] M.C. Drake, and G.M. Rosenblatt, "Rotational Raman Scattering from Premixed and Diffusion Flames," *Combust. Flame* **33**, 179–196, (1978).

[12] B.J. McBride, and S. Gordon, "Computer Program for Calculation of Complex Chemical Equilibrium Compositions and Applications – II. Users Manual and Program Description," NASA RP–1311, (1996).

[13] I.S. Dring, R. Devonshire, J. Meads, H.F. Boysan, D.A. Greenhalgh, "Observation of Non-Equilibrium Effects in Free-Convective Flows Using CARS. Recirculating Flow Relaxation Spectrometry," *Chem. Phys. Lett.* **132**, 283–290, (1986).

[14] C. Eckbreth, *Laser Diagnostics for Combustion Temperature and Species*: 2nd Ed., Gordon and Breach Publishers, The Netherlands, 97–98, (1996).

[15] *Private-communication*, A. Iannetti. Combustor simulations were performed using NASA's National Combustor Code (NCC), (2003).

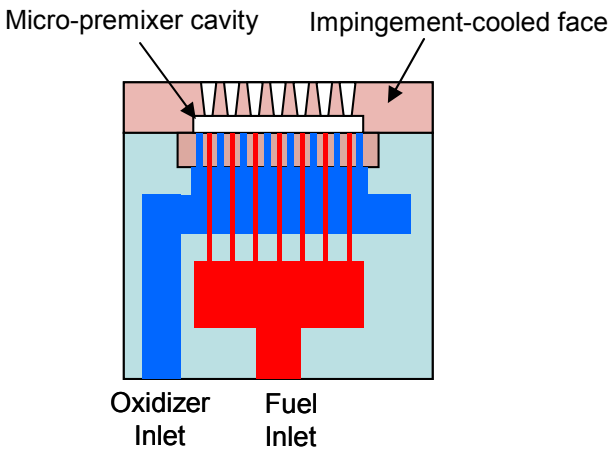


Figure 1: A schematic of the burner nozzle design.

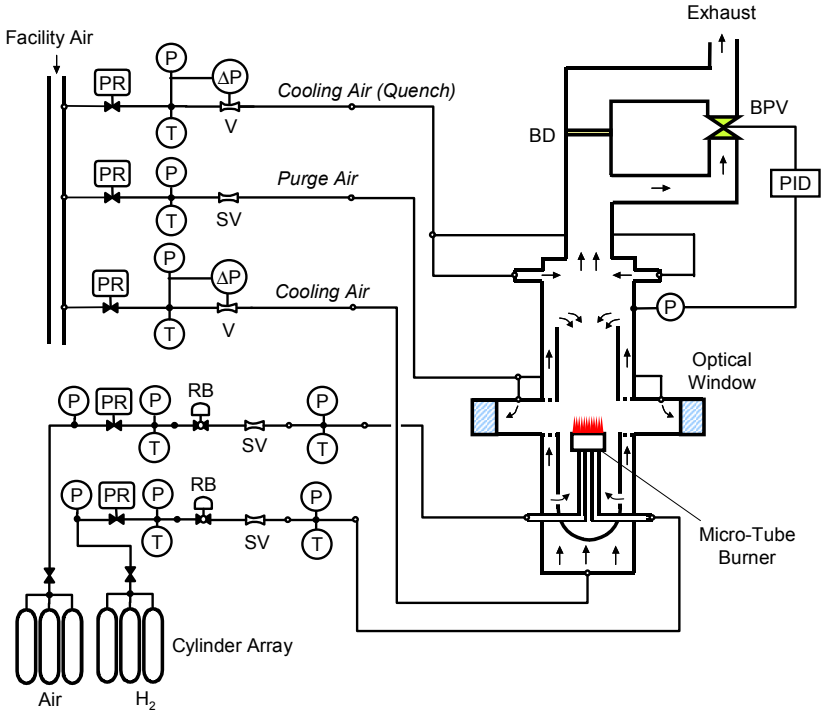


Figure 2: High-pressure gaseous burner rig and gas flow system for up to 30-atm combustion. P: pressure transducer; T: thermocouple; PR: remotely operated regulator; RB: remotely operated ball valve; V: venturi; SV: sonic venturi; BPV: back-pressure valve; PID: process controller; BD: burst disk.

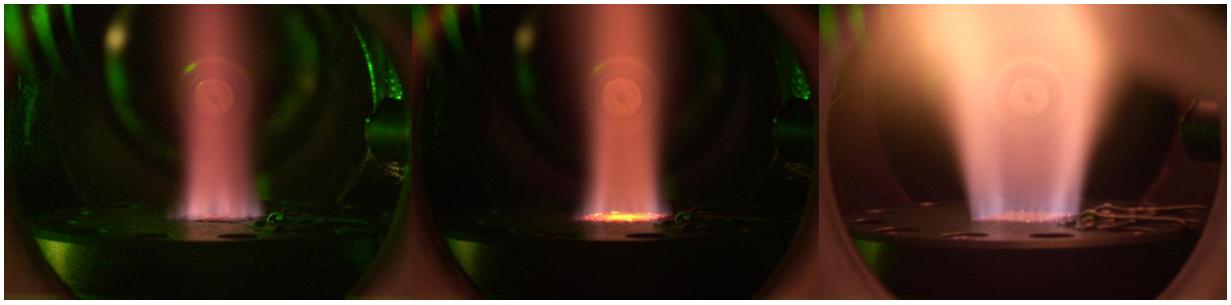

(a) $\phi$ = 0.6 (b) $\phi$ = 1.0 (c) $\phi$ = 3.2

Figure 3: Photographs of $H_2$-air premixed flames at 10 atm. In 3b the burner face glows due to high surface temperature (~700 K). The images of light-collecting fiber optics appear in photos through the flame images, which center (fiber core position) indicate the measurement height.

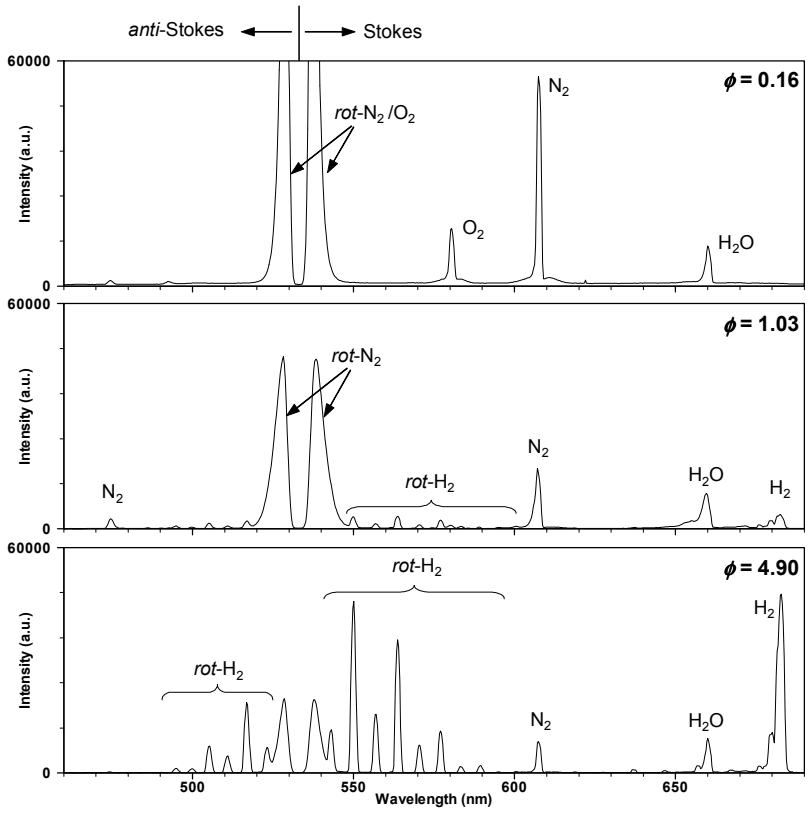


Figure 4: Spontaneous Raman spectra in 10-atm $H_2$-air combustion (300-shot averaged). Note the overall air flow rates for $\phi$ = 0.16, 1.03, and 4.90 are 328, 259, and 98 SLM, respectively due to practical operating reasons. Accordingly, the integrated intensity of $N_2$ Raman decreases as $\phi$ increases.

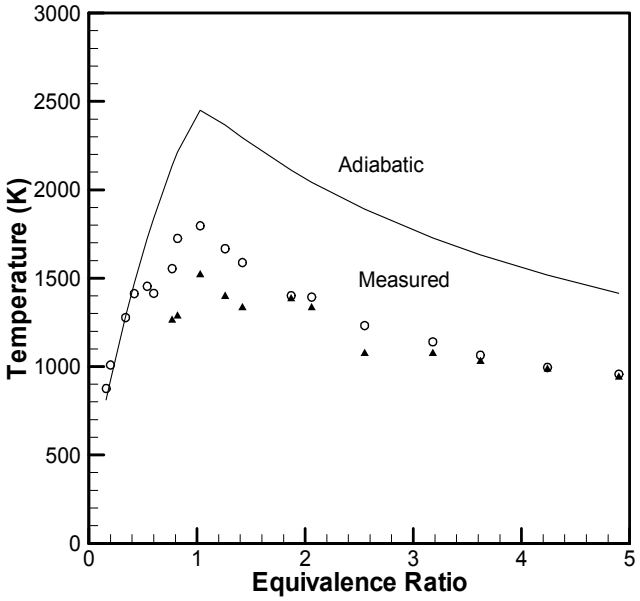


Figure 5: Measured temperature in 10-atm $H_2$-air combustion via Raman spectra. *Circle* (white) is anti-Stokes/Stokes temperature; *Triangle* (black) is rotational $H_2$ temperature. *Solid line* is adiabatic temperature via CEA code.

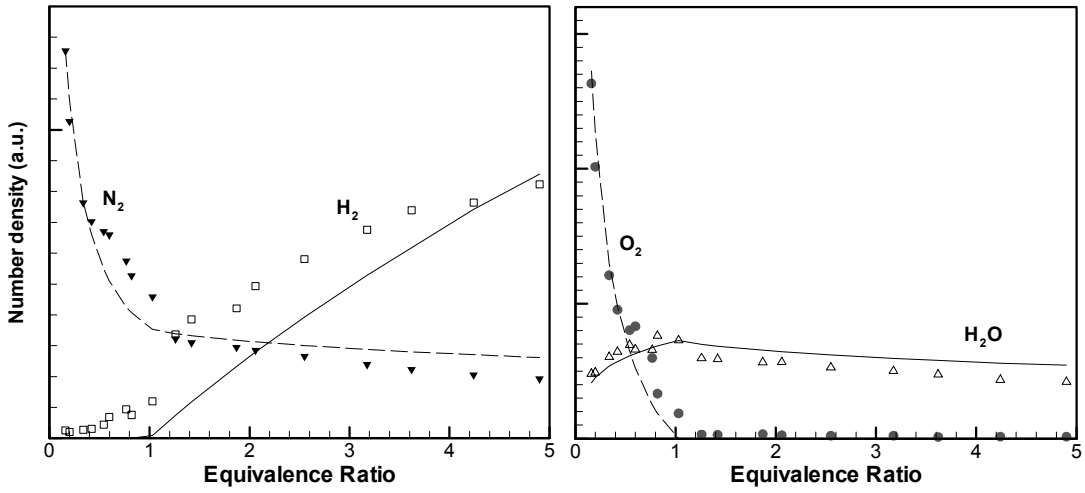


Figure 6: Quantitative comparison of measured species concentration with calculated results in 10-atm $H_2$-air combustion. *Solid* and *dashed lines* are adiabatic calculation; *Dots* are experimental data. Experimental data points are fitted to calculated profiles at the maximum value. Calculated results are based on CEA calculation with assigned experimental temperature (Stokes/anti-Stokes temperature).

# REPORT DOCUMENTATION PAGE

*Form Approved*
*OMB No. 0704-0188*



| 1. AGENCY USE ONLY (*Leave blank*) | 2. REPORT DATE | 3. REPORT TYPE AND DATES COVERED |
|---|---|---|
| | December 2003 | Technical Memorandum |

**4. TITLE AND SUBTITLE**

Development of a High-Pressure Gaseous Burner for Calibrating Optical Diagnostic Techniques

**5. FUNDING NUMBERS**

WBS–22–714–02–16

**6. AUTHOR(S)**

Jun Kojima and Quang-Viet Nguyen

**7. PERFORMING ORGANIZATION NAME(S) AND ADDRESS(ES)**

National Aeronautics and Space Administration
John H. Glenn Research Center at Lewis Field
Cleveland, Ohio 44135–3191

**8. PERFORMING ORGANIZATION REPORT NUMBER**

E–14263

**9. SPONSORING/MONITORING AGENCY NAME(S) AND ADDRESS(ES)**

National Aeronautics and Space Administration
Washington, DC 20546–0001

**10. SPONSORING/MONITORING AGENCY REPORT NUMBER**

NASA TM—2003-212738

**11. SUPPLEMENTARY NOTES**

Prepared for the 2003 American Flame Research Committee International Symposium on Combustion Research and Industrial Practice: Bridging the Gap cosponsored by the American Flame Research Committee (AFRC) and the Combustion Research Facility of Sandia National Laboratory, Livermore, California, October 16–17, 2003. Jun Kojima, Ohio Aerospace Institute, Brook Park, Ohio 44142 and National Research Council—NASA Resident Research Associate at Glenn Research Center; and Quang-Viet Nguyen, NASA Glenn Research Center. Responsible person, Quang-Viet Nguyen, organization code 5830, 216–433–3574.

**12a. DISTRIBUTION/AVAILABILITY STATEMENT**

Unclassified - Unlimited
Subject Categories: 07, 18, 28, 44 and 77 Distribution: Nonstandard

Available electronically at http://gltrs.grc.nasa.gov

This publication is available from the NASA Center for AeroSpace Information, 301–621–0390.

**12b. DISTRIBUTION CODE**

**13. ABSTRACT** ***(Maximum 200 words)***

In this work-in-progress report, we show the development of a unique high-pressure burner facility (up to 60 atm) that provides steady, reproducible premixed flames with high precision, while having the capability to use multiple fuel/oxidizer combinations. The high-pressure facility has four optical access ports for applying different laser diagnostic techniques and will provide a standard reference flame for the development of a spectroscopic database in high-pressure/temperature conditions. Spontaneous Raman scattering (SRS) was the first diagnostic applied, and was used to successfully probe premixed hydrogen-air flames generated in the facility using a novel multi-jet micro-premixed array burner element. The SRS spectral data include contributions from $H_2$, $N_2$, $O_2$, and $H_2O$ and were collected over a wide range of equivalence ratios ranging from 0.16 to 4.9 at an initial pressure of 10-atm via a spatially resolved point SRS measurement with a high-performance optical system. Temperatures in fuel-lean to stoichiometric conditions were determined from the ratio of the Stokes to anti-Stokes scattering of the *Q*-branch of $N_2$, and those in fuel-rich conditions via the rotational temperature of $H_2$. The SRS derived temperatures using both techniques were consistent and indicated that the flame temperature was approximately 500 K below that predicted by adiabatic equilibrium, indicating a large amount of heat-loss at the measurement zone. The integrated vibrational SRS signals show that SRS provides quantitative number density data in high-pressure $H_2$-air flames.

**14. SUBJECT TERMS**

Temperature measurement; Nonintrusive measurement; Hydrogen fuels; Turbulent combustion; Combustion temperature; Combustion physics; Flame spectroscopy; Molecular spectroscopy; Raman spectroscopy

**15. NUMBER OF PAGES**

19

**16. PRICE CODE**

| 17. SECURITY CLASSIFICATION OF REPORT | 18. SECURITY CLASSIFICATION OF THIS PAGE | 19. SECURITY CLASSIFICATION OF ABSTRACT | 20. LIMITATION OF ABSTRACT |
|---|---|---|---|
| Unclassified | Unclassified | Unclassified | |